Exact Ansatz of Fermion-Boson Systems for a Quantum Device

Samuel Warren,[1] Yuchen Wang,[1] Carlos L. Benavides-Riveros,[2,*] and David A. Mazziotti[1,†]

[1]*Department of Chemistry and The James Franck Institute, The University of Chicago, Chicago, Illinois 60637, USA*

[2]*Pitaevskii BEC Center, CNR-INO and Dipartimento di Fisica, Università di Trento, I-38123 Trento, Italy*

(Dated: Submitted February 16, 2024; Revised May 13, 2024; Revised July 12, 2024)

We present an exact ansatz for the eigenstate problem of mixed fermion-boson systems that can be implemented on quantum devices. Based on a generalization of the electronic contracted Schrödinger equation (CSE), our approach guides a trial wave function to the ground state of any arbitrary mixed Hamiltonian by directly measuring residuals of the mixed CSE on a quantum device. Unlike density-functional and coupled-cluster theories applied to electron-phonon or electron-photon systems, the accuracy of our approach is not limited by the unknown exchange-correlation functional or the uncontrolled form of the exponential ansatz. To test the performance of the method, we study the Tavis-Cummings model, commonly used in polaritonic quantum chemistry. Our results demonstrate that the CSE is a powerful tool in the development of quantum algorithms for solving general fermion-boson many-body problems.

Introduction.— Strong coupling with bosonic particles can drastically change many physical properties of electronic systems. For instance, when coupled with phonons, low-energy electronic excitations are strongly modified, influencing, as a result, the optical, thermodynamic, and transport properties of solids [1]. This electron-phonon coupling is also the source of the effective attractive electronic interaction needed for conventional superconductivity [2, 3]. When coupled with light, emergent hybrid quantum states (known as polaritons) can catalyze or inhibit the reactive paths of chemical reactions [4–7]. Both electron-phonon and electron-photon couplings lead to many fascinating chemical and technological applications, including spintronics [8], quantum information processing [9, 10], optical control of collective modes in solids [11], catalysis [12–14], solar power [15], or low energy lasing [16–19].

Given the complexity of these entangled electron-boson systems, it is not surprising that their theoretical description usually relies on semi-empirical model Hamiltonians [20–23]. However, a more complete understanding of the effects arising from mixed particle coupling requires quantitative methods that treat electronic and bosonic modes with equal theoretical rigor [24–27]. For instance, to predict reaction pathways in polaritonic catalysis, it is important to port over electronic structure methods to mixed fermion-boson problems [28]. Current ab-initio approaches are mainly variants of density functional theory (DFT), and, while lattice dynamics and electron-photon coupling can be accounted for through perturbative [29–31] or quantum electrodynamics DFT [28, 32, 33], the unknown form of the corresponding exchange-correlation functionals for the electron-boson interaction limits the accuracy of both approaches [34–36]. Alternative methods can be found in a new class of coupled cluster (CC) algorithms. Originally developed for electrons [37, 38], CC has been extended to electron-phonon [39] and electron-photon [40–42] systems, where the key ingredient is an exponential ansatz that approximates higher-body excitations in terms of products of lower-body excitations. Recently, inspired by the prospects of quantum computing, there has been considerable development of CC's unitary form [43–46]. In both cases the accuracy of the approach strongly depends on the excitation level in the ansatz. In addition, from the quantum computational viewpoint, its Trotterized implementation is not always well defined [47].

Here we report the development of an alternative approach that gives an exact ansatz for ground and excited states of arbitrary electron-boson systems, overcoming the limitations of both DFT and CC methods. Our approach is based on an extension of the contracted Schrödinger equation (CSE) [48–66], known in the context of reduced density matrix theory for fermionic systems [67–69]. Our main result is an exact ansatz that can be implemented directly on quantum devices to find the eigenstates of arbitrary mixed particle Hamiltonians.

The Letter is structured as follows. First, we recap and extend the fermionic CSE to general many-body physics, including boson-fermion systems. We then discuss how the CSE ansatz can inform a quantum algorithm for finding the ground states of mixed particle systems. In the second part of the paper, we demonstrate the effectiveness of the CSE ansatz on the Tavis-Cummings model. Finally, we discuss potential future directions and the implications of our results.

Theory.— Originally derived for fermionic systems, the *Contracted Schrödinger Equation* (CSE) reads [48–59]:

$$\langle\Psi|\, \hat{a}^\dagger_{i_1} \hat{a}^\dagger_{i_2} \hat{a}_{k_2} \hat{a}_{k_1} \hat{H}\, |\Psi\rangle = E\ {}^2D^{i_1 i_2}_{k_1 k_2} \tag{1}$$

where $\hat{a}^\dagger_i$ and $\hat{a}_k$ are fermionic creation and annihilation operators on the $i^{\rm th}$ and $k^{\rm th}$ sites, respectively, and

$${}^2D^{i_1 i_2}_{k_1 k_2} = \langle\Psi|\, \hat{a}^\dagger_{i_1} \hat{a}^\dagger_{i_2} \hat{a}_{k_2} \hat{a}_{k_1} |\Psi\rangle \tag{2}$$

is the two-body reduced density matrix (RDM). Nakatsuji's theorem states that the CSE (1) is satisfied if and only if the corresponding N-body preimage of ${}^2D^{i_1 i_2}_{k_1 k_2}$ satisfies the usual Schrödinger equation (SE) [48, 58].

We now extend the CSE to mixed fermion-boson systems and show that Nakatsuji's theorem also holds for those systems. Let's first define a general electron-boson density operator

$$\hat{\Gamma}^{i_1\ldots i_q, j_1\ldots j_s}_{k_1\ldots k_r, l_1\ldots l_t} = \hat{a}^\dagger_{i_1}\ldots\hat{a}^\dagger_{i_q}\hat{a}_{k_r}\ldots\hat{a}_{k_1}\hat{b}^\dagger_{j_1}\ldots\hat{b}^\dagger_{j_s}\hat{b}_{l_t}\ldots\hat{b}_{l_1} \equiv \hat{\Gamma}^{\boldsymbol{i},\boldsymbol{j}}_{\boldsymbol{k},\boldsymbol{l}}, \quad (3)$$

where $\hat{b}^\dagger_j$ and $\hat{b}_l$ are bosonic creation and annihilation operators. Here i_m and k_m (j_m and l_m) run over the different fermionic (bosonic) indices, and we use the compact notation $\boldsymbol{i} = (i_1, ..., i_q)$, $\boldsymbol{k} = (k_1, ..., k_r)$, $\boldsymbol{j} = (j_1, ..., j_s)$ and $\boldsymbol{l} = (l_1, ..., l_t)$.

The density operator (3) allows us to define concisely a general fermion-boson (fb) Hamiltonian:

$$\hat{H}_{fb} = \sum_{\boldsymbol{ik},\boldsymbol{jl}} h^{\boldsymbol{i},\boldsymbol{j}}_{\boldsymbol{k},\boldsymbol{l}} \hat{\Gamma}^{\boldsymbol{i},\boldsymbol{j}}_{\boldsymbol{k},\boldsymbol{l}}. \quad (4)$$

We then multiply the corresponding fermion-boson SE, i.e., $\hat{H}_{fb}|\Psi\rangle = E|\Psi\rangle$, on the left by $\langle\Psi|\hat{\Gamma}^{\boldsymbol{i},\boldsymbol{j}}_{\boldsymbol{k},\boldsymbol{l}}$ to obtain a *generalized* CSE:

$$\langle\Psi|\hat{\Gamma}^{\boldsymbol{i},\boldsymbol{j}}_{\boldsymbol{k},\boldsymbol{l}}\hat{H}_{fb}|\Psi\rangle = ED^{\boldsymbol{i},\boldsymbol{j}}_{\boldsymbol{k},\boldsymbol{l}}, \quad (5)$$

where $D^{\boldsymbol{i},\boldsymbol{j}}_{\boldsymbol{k},\boldsymbol{l}} = \langle\Psi|\hat{\Gamma}^{\boldsymbol{i},\boldsymbol{j}}_{\boldsymbol{k},\boldsymbol{l}}|\Psi\rangle$ is a *generalized* RDM of the electron-boson system. Multiplying both sides of the generalized CSE (5) by the elements of the reduced Hamiltonian matrix $h^{\boldsymbol{i},\boldsymbol{j}}_{\boldsymbol{k},\boldsymbol{l}}$ and summing over all indices yields

$$\sum_{\boldsymbol{ik},\boldsymbol{jl}} h^{\boldsymbol{i},\boldsymbol{j}}_{\boldsymbol{k},\boldsymbol{l}}\langle\Psi|\hat{\Gamma}^{\boldsymbol{i},\boldsymbol{j}}_{\boldsymbol{k},\boldsymbol{l}}\hat{H}_{fb}|\Psi\rangle = E\sum_{\boldsymbol{ik},\boldsymbol{jl}} h^{\boldsymbol{i},\boldsymbol{j}}_{\boldsymbol{k},\boldsymbol{l}} D^{\boldsymbol{i},\boldsymbol{j}}_{\boldsymbol{k},\boldsymbol{l}}. \quad (6)$$

The sum on the right-hand side is equal to the energy, making the expression equal to E^2. Thus, the equation can be rewritten as the energy variance

$$\langle\Psi|\hat{H}^2_{fb}|\Psi\rangle - \langle\Psi|\hat{H}_{fb}|\Psi\rangle^2 = 0, \quad (7)$$

which, as a stationary condition for the wave function, is equivalent to the SE. Therefore, the set of solutions to Eq. (5) must be the same as the solutions to the electron-boson SE. This derivation shows that the minimal RDM necessary to satisfy both the CSE and SE will have the same degrees of freedom as the corresponding many-body Hamiltonian. This is reminiscent of the standard electronic structure problem where a nondegenerate electronic ground-state wavefunction maps to a unique 2-electron RDM, which, as a result, has enough information to build higher-order RDMs and the exact wavefunction [48, 70].

The CSE (5) can be further decomposed into Hermitian and anti-Hermitian parts:

$$\langle\Psi|\hat{\Gamma}(\hat{H}_{fb} - E))|\Psi\rangle = \frac{1}{2}\big(\langle\Psi|[\hat{\Gamma}, \hat{H}_{fb}]|\Psi\rangle + \langle\Psi|\{\hat{\Gamma}, \hat{H}_{fb} - E\}|\Psi\rangle\big), \quad (8)$$

where $[\cdot,\cdot]$ and $\{\cdot,\cdot\}$ are the usual commutator and anticommutator. As described in several prior works for the electronic problem, this decomposition can be used to converge to stationary states either through classical [60–66, 71] or quantum [56, 72–77] computing methods.

On modern quantum devices, the *Contracted Quantum Eigensolver* (CQE) algorithm measures the total residual of Eq. (8) for trial wave functions. Such a residual can then be used to guide a sequence of trial wave functions toward the ground (or an eigen-) state by iteratively applying a sequence of exponential transformations. The scheme is agnostic to the statistics of the system and has already been applied both for fermions and bosons with significant success [56, 73–77]. Here, we will show that the CQE algorithms also provide a simple methodology for resolving the ground state in mixed fermion-boson systems.

Our scheme is as follows: at iteration $(n+1)$ the wave function results from two separate exponential transformations of the wave function at iteration (n) [56]:

$$|\Psi^{(n+1)}\rangle = \exp(\eta_B\hat{B}^{(n)})\exp(\eta_A\hat{A}^{(n)})|\Psi^{(n)}\rangle, \quad (9)$$

where

$$\hat{A}^{(n)} = \sum_{\boldsymbol{ik},\boldsymbol{jl}} A^{(n)}_{\boldsymbol{ik},\boldsymbol{jl}}\hat{\Gamma}^{\boldsymbol{i},\boldsymbol{j}}_{\boldsymbol{k},\boldsymbol{l}} \quad (10)$$

is an anti-Hermitian operator,

$$\hat{B}^{(n)} = \sum_{\boldsymbol{ik},\boldsymbol{jl}} B^{(n)}_{\boldsymbol{ik},\boldsymbol{jl}}\hat{\Gamma}^{\boldsymbol{i},\boldsymbol{j}}_{\boldsymbol{k},\boldsymbol{l}} \quad (11)$$

is a Hermitian one, and η_A and η_B can be interpreted as learning rates of the algorithm.

Notice that if the unitary operator $\exp(\eta_A\hat{A}^{(n)})$ is applied to a normalized wave function $|\Psi^{(n)}\rangle$, the total energy of the transformed state is (in leading order of the parameter η_A): $\mathcal{E}_{n+1} = \mathcal{E}_n + \eta_A\langle\Psi^{(n)}|[\hat{H}_{fb}, \hat{A}^{(n)}]|\Psi^{(n)}\rangle + \mathcal{O}(\eta_A^2)$ where $\mathcal{E}_n = \langle\Psi^{(n)}|\hat{H}_{fb}|\Psi^{(n)}\rangle$. As a result, the anti-Hermitian portion of Eq. (8) can be used as a residual to find the optimal operator at each step, and the anti-Hermitian parameters can be updated as follows:

$$A^{(n)} = \langle\Psi^{(n)}|[\hat{\Gamma}, \hat{H}_{fb}]|\Psi^{(n)}\rangle. \quad (12)$$

These parameters generate the unitary $\exp(\eta_A\hat{A}^{(n)})$. In turn, η_A can be selected to minimize the expectation energy of the resulting state $|\Phi^{(n)}\rangle = \exp(\eta_A\hat{A}^{(n)})|\Psi^{(n)}\rangle$. Quite remarkably, many well-known canonical transformations of mixed fermion-boson systems are exactly recovered when only the anti-Hermitian part of the ansatz is used. This is the case, for instance, of the Lang-Firsov transformation for the Holstein Hamiltonian [78] or the Schrieffer-Wolff transformation for the Anderson model [79]. As already suggested for the electronic case [71], this means that the anti-Hermitian part of the CSE converges to the appropriate canonical transformation of the respective problem.

Next, the Hermitian portion of the residual is measured with respect to the updated (normalized) vector $|\Phi^{(n)}\rangle$.

$$B^{(n)} = \langle\Phi^{(n)}| \{\hat{\Gamma}, \hat{H}_{fb} - E^{(n)}\} |\Phi^{(n)}\rangle \,, \qquad (13)$$

where $E^{(n)} = \langle\Phi^{(n)}| \hat{H}_{fb} |\Phi^{(n)}\rangle$. The resulting Hermitian operator $\hat{B}^{(n)}$ generates the non-unitary $\exp(\eta_B \hat{B}^{(n)})$ where η_B is selected to minimize the energy of $|\Psi^{(n+1)}\rangle$. Implementing non-unitary operators on quantum devices is an active field of research [80, 81] and has resulted in the development of several methods such as quantum imaginary-time evolution [82, 83]. Prior implementations of the fermionic CQE have utilized dilation techniques similar to the Sz.-Nagy dilation [56], but the CQE is agnostic to the particular technique used to accomplish non-unitary transformations. Here, we exactly map the non-unitary transformation to a unitary transformation on a classical device, allowing us to focus on the effectiveness of the CSE ansatz for mixed systems.

The CSE ansatz (e.g., Eq. (9)) is a product-of-exponentials ansatz whose gradient by construction equals the residual of the CSE or its Hermitian and anti-Hermitian components [55, 56, 71]. It has some important differences from other ansätze such as those from unitary coupled cluster (UCC) theory [84], generalized coupled cluster (GCC) theory [85, 86], and quantum imaginary time evolution (QITE) [87]. If the non-unitary part of the CSE ansatz is removed, we obtain the anti-Hermitian CSE (ACSE) ansatz [61] whose gradient equals the residual of the ACSE. Like the ACSE, the UCC is a unitary ansatz, but unlike the ACSE, it contains a single exponential of only occupied-to-unoccupied-orbital transitions [84]. The disentangled UCC ansatz [88], whose truncations are unequal to those of the UCC ansatz, introduces a product of exponential operators like the ACSE but retains the restriction to only occupied-to-unoccupied-orbital transitions.

If the unitary part of the CSE ansatz is removed, we obtain the Hermitian CSE (HCSE) ansatz [55, 56, 71] whose gradient equals the residual of the HCSE. Like the HCSE, the GCC is a non-unitary ansatz, but unlike the HCSE, it contains only a single exponential operator [85, 86]. While the GCC was initially conjectured to be exact [86], it was later shown to be an approximation [71]. The CSE and HCSE ansätze were introduced to generalize GCC to satisfy the CSE and HCSE equations upon convergence, respectively [55, 71], and hence, to be verifiably exact [56]. Finally, restricting the two-body operator of each exponential in the HCSE to be the Hamiltonian yields QITE [87, 89]. This restriction significantly slows the convergence of the exponential product from linear (or superlinear in a quasi-Newton optimization) [90] to an exponential decay that depends upon the energy gap between the ground and excited states.

We note that because the gradient of the CSE ansatz equals the residual of the CSE, gradient descent (or quasi-Newton optimization) provides linear (or superlinear) convergence [91] to a solution of the CSE, which is a solution of the Schrödinger equation. For a comparison of the convergence rates of the CSE, HCSE, and ACSE in molecular cases, refer to Ref. [56].

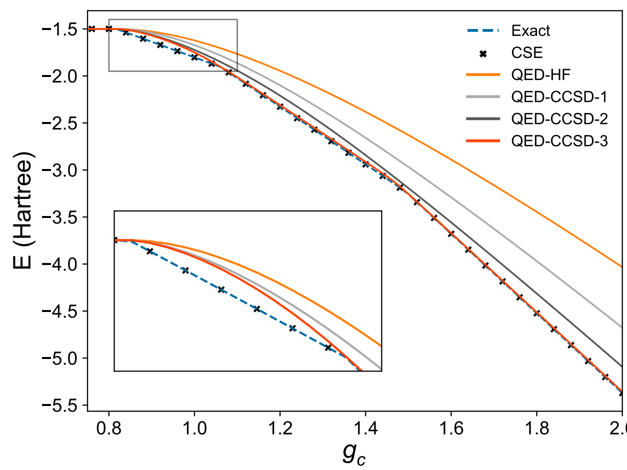

FIG. 1. CSE and QED-CCSD energies for the 3 fermion Tavis-Cummings model with increasing coupling. The Hamiltonian parameters from Eq. (14) were fixed as $(\omega_b, \omega_f) = (2, 0.5)$ while g_c is varied as shown along the x-axis. The QED-CCSD-n methods are named according to the convention used in Ref. [41].

To study the numerical performance of the algorithm, we use the *Tavis-Cummings model* (TC). This is a prototypical mixed fermion-boson system that attempts to capture the behavior of polaritons in a wide range of coupling regimes [92–96]. The model is comprised of N two-level fermionic systems coupled to a bosonic mode, making it analogous to situations found in polaritonic chemistry where molecules are bound in cavities [6, 13, 26, 97] or solid-state intersubband devices [98, 99]. The TC Hamiltonian is written as follows:

$$\hat{H} = \omega_b \hat{b}^\dagger \hat{b} + \sum_{i=1}^{N} \left[\omega_f \hat{a}^\dagger_{i+} \hat{a}_{i+} + g_c \big(\hat{a}^\dagger_{i+} \hat{a}_{i-} \hat{b} + \hat{a}^\dagger_{i-} \hat{a}_{i+} \hat{b}^\dagger \big) \right] , \qquad (14)$$

with the fermionic subscripts indicating the excited (+) and ground (−) orbitals in the i^{th} two-level system, and where ω_b, ω_f, and g_c describe the angular frequency of the bosonic mode, the transition frequency of the fermionic modes, and the coupling between the bosonic mode and the fermionic bath, respectively. The TC Hamiltonian contains no explicit fermionic correlation, but, due to the mixed particle coupling, significant correlation exists between the bosonic and fermionic degrees of freedom, which renders mean field methods, like quantum electrodynamics Hartree-Fock (QED-HF), ineffective.

Results.— We first compare the CQE ground-state results to those obtained from the mixed fermion-boson

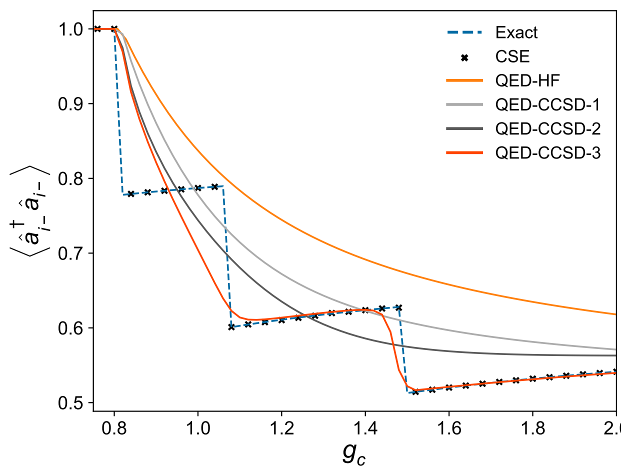

FIG. 2. CSE and QED-CCSD predicted ground fermionic orbital populations with increasing coupling in the 3-fermion Tavis-Cummings Model.

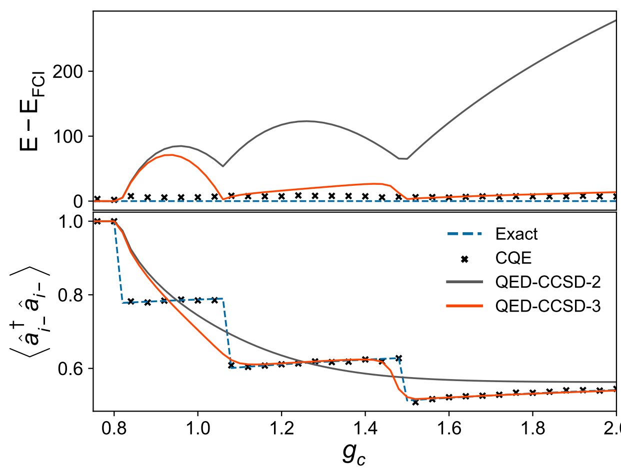

FIG. 3. CQE and QED-CCSD ground-state energy and fermionic orbital population with increasing coupling. The y-axis of the energy shows the absolute error in mHartree.

quantum electrodynamics coupled cluster (QED-CC) methods for the TC model. Those are named such that QED-CC(SD)-n refers to coupled-cluster with single and double fermionic cluster terms combined with bosonic and mixed cluster terms containing up to n bosonic creation operators [41].

Fig. 1 depicts the ground-state energies predicted by various methods for the 3-site TC model as the coupling strength increases, entering well into the ultra-strong regime. The QED-CC methods capture the general trend of the energies but do not align with any section of the exact energy curve, including the high-level QED-CCSD-3. The QED-CCSD-3 is the most accurate QED-CCSD method possible for the coupling strength shown in the figure at which only single, double, and triple bosonic excitations contribute to the exact ground state. This suggests that QED-CCSD-3 would begin to fail again in the stronger coupling limit when the maximum bosonic population increases to 4 or larger. Additionally, despite being the best CCSD method in this region, QED-CCSD-3 is unable to predict the transition in the weak coupling limit seen in the zoomed-in section of the figure due to the omission of the triple cluster operator. The CSE, however, is able to accurately reproduce the exact energy regardless of coupling strength. Notice that this accuracy is achieved while only ever measuring the residual with the same density operators that appear in the TC Hamiltonian, while QED-CC must include all possible excitations to be accurate. Therefore, while the number of bosonic and mixed cluster terms remains fixed for the CQE, for the QED-CC methods it will grow with the coupling strength or, equivalently, the maximum boson population.

Fig. 2 demonstrates how QED-CC methods fail to capture both the quantitative and qualitative properties of the TC model. The plot shows the predicted population of the lower energy level in any of the fermionic two-level subsystems, which, due to symmetry, are the same. The QED-CC methods up to QED-CCSD-2 approximate the discontinuous population changes with successively better least squares errors, but fail to capture any of the stair-stepping behavior caused by actual level crossings. QED-CCSD-3 smoothes out the final two stair steps, but completely misses the first, as could be predicted from its failure in the prior figure. The CSE method, however, exactly recovers the populations, despite needing to resolve nearly degenerate states at the level crossings. The failure of CC to resolve level crossings [100] and the success of the CSE highlight the importance of the particular combination of Hermitian and anti-Hermitian contributions present in the CSE ansatz.

Finally, Fig. 3 compares the results from the CQE algorithm performed on an ideal quantum device simulator to those obtained from classical QED-CCSD. The CQE algorithm reproduces the energies with an average error of 7 mhartree with a standard deviation of 1 mhartree, indicating that the error is uniform regardless of the distance from the level crossings. This is in contrast to the CC methods where the error exhibits significant fluctuations. The CQE recovers the ground orbital populations near the degeneracies despite not exactly recovering the energy. These results demonstrate that despite sampling error, due to the finite number of measurements (shots) on a quantum device simulator, the CQE is able to outperform some of the most popular classical algorithms for mixed-particle systems.

Conclusions.— Based on a generalization of the electronic CSE, we present an exact ansatz for mixed quantum fermion-boson systems. Our numerical results on the Tavis-Cumming model demonstrate the power of the CSE ansatz. While CC methods require constantly increasing the number of terms in the exponential to be accurate in different coupling regimes, the CSE is always exact and the required number of terms exactly matches the density operators present in the Hamiltonian. Additionally, the CQE demonstrates how the CSE can be applied on a quantum device, and can outperform cutting-edge classical algorithms. This Letter leaves many avenues for future works, whether it be the development of classical computing algorithms for mixed particle systems that leverage the CSE or the application of the CQE on real quantum devices. For example, molecular systems coupled to a bath, such as those found in polaritonic chemistry, will be explored in future work. Furthermore, since the ansatz can be equally used for any eigenstate [101], the computation of exact excited states in polaritonic quantum chemistry is also a promising future direction.

D.A.M. gratefully acknowledges the U.S. Department of Energy, Office of Basic Energy Sciences, Grant DE-SC0019215, and the U.S. National Science Foundation (NSF) Grant No. CHE-2155082 and the NSF RAISE-QAC-QSA Grant No. DMR-2037783. C.L.B.-R. gratefully thanks Daniele De Bernardis and Jorge Campos, for insightful discussions and acknowledges financial support from the European Union's Horizon Europe Research and Innovation program under the Marie Skłodowska-Curie Grant Agreement n°101065295–RDMFTforbosons. Views and opinions expressed are however those of the author only and do not necessarily reflect those of the European Union or the European Research Executive Agency.

* cl.benavidesriveros@unitn.it
† damazz@uchicago.edu

[1] J. Ziman, *Electrons and Phonons: The Theory of Transport Phenomena in Solids* (Oxford University Press, 2001).
[2] H. Fröhlich, Electrons in lattice fields, Adv. Phys. **3**, 325 (1954).
[3] J. Bardeen, L. N. Cooper, and J. R. Schrieffer, Theory of superconductivity, Phys. Rev. **108**, 1175 (1957).
[4] F. J. Garcia-Vidal, C. Ciuti, and T. W. Ebbesen, Manipulating matter by strong coupling to vacuum fields, Science **373**, eabd0336 (2021).
[5] T. W. Ebbesen, Hybrid light–matter states in a molecular and material science perspective, Acc. Chem. Res **49**, 2403 (2016).
[6] R. Ribeiro, L. A. Martínez-Martínez, M. Du, J. Campos-Gonzalez-Angulo, and J. Yuen-Zhou, Polariton Chemistry: Controlling Molecular Dynamics with Optical Cavities, Chem. Sci. **9**, 6325 (2018).
[7] A. Thomas, J. George, A. Shalabney, M. Dryzhakov, S. Varma, J. Moran, T. Chervy, X. Zhong, E. Devaux, C. Genet, J. A. Hutchison, and T. Ebbesen, Ground-State Chemical Reactivity under Vibrational Coupling to the Vacuum Electromagnetic Field, Angew. Chem. Int. Ed. **55**, 11462 (2016).
[8] S. Mondal and A. Lunghi, Spin-phonon decoherence in solid-state paramagnetic defects from first principles, npj Comput. Mater. **9**, 120 (2023).
[9] K. Jahnke, A. Sipahigil, J. Binder, M. Doherty, M. Metsch, L. Rogers, N. Manson, M. Lukin, and F. Jelezko, Electron–phonon processes of the silicon-vacancy centre in diamond, New J. Phys. **17**, 043011 (2015).
[10] T. D. Ladd, F. Jelezko, R. Laflamme, Y. Nakamura, C. Monroe, and J. L. O'Brien, Quantum computers, Nature **464**, 45 (2010).
[11] J. Bloch, A. Cavalleri, V. Galitski, M. Hafezi, and A. Rubio, Strongly correlated electron–photon systems, Nature **606**, 41 (2022).
[12] J. Campos-Gonzalez-Angulo, R. Ribeiro, and J. Yuen-Zhou, Resonant Catalysis of Thermally Activated Chemical Reactions with Vibrational Polaritons, Nat. Commun. **10**, 4685 (2019).
[13] S. Kéna-Cohen and J. Yuen-Zhou, Polariton Chemistry: Action in the Dark, ACS Cent. Sci. **5**, 386 (2019).
[14] M. Du and J. Yuen-Zhou, Catalysis by Dark States in Vibropolaritonic Chemistry, Phys. Rev. Lett. **128**, 096001 (2022).
[15] M. Farhat, A. Baloch, S. Rashkeev, N. Tabet, S. Kais, and F. Alharbi, Bifacial Schottky-Junction Plasmonic-Based Solar Cell, Energy Technol. **8**, 1901280 (2020).
[16] A. Imamoglu, R. Ram, S. Pau, and Y. Yamamoto, Nonequilibrium condensates and lasers without inversion: Exciton-polariton lasers, Phys. Rev. A **53**, 4250 (1996).
[17] H. Deng, G. Weihs, D. Snoke, J. Bloch, and Y. Yamamoto, Polariton Lasing vs. Photon Lasing in a Semiconductor Microcavity, Proc. Natl. Acad. Sci. U.S.A. **100**, 15318 (2003).
[18] S. Kim, B. Zhang, Z. Wang, J. Fischer, S. Brodbeck, M. Kamp, C. Schneider, S. Höfling, and H. Deng, Coherent Polariton Laser, Phys. Rev. X **6**, 011026 (2016).
[19] M. Leng, J. Wu, K. Dini, J. Liu, Z. Hu, J. Tang, T. C. H. Liew, H. Sun, R. Su, and Q. Xiong, Optically Pumped Polaritons in Perovskite Light-Emitting Diodes, ACS Photonics **10**, 1349 (2023).
[20] F. Giustino, Electron-phonon interactions from first principles, Rev. Mod. Phys. **89**, 015003 (2017).
[21] H. Walther, B. Varcoe, B.-G. Englert, and T. Becker, Cavity quantum electrodynamics, Rep. Prog. Phys. **69**, 1325 (2006).
[22] J. Levinsen, F. Marchetti, J. Keeling, and M. Parish, Spectroscopic Signatures of Quantum Many-Body Correlations in Polariton Microcavities, Phys. Rev. Lett. **123**, 266401 (2019).
[23] L. Tan, O. Diessel, A. Popert, R. Schmidt, A. Imamoglu, and M. Kroner, Bose Polaron Interactions in a Cavity-Coupled Monolayer Semiconductor, Phys. Rev. X **13**, 031036 (2023).
[24] H. Spohn, *Dynamics of Charged Particles and their Radiation Field* (Cambridge University Press, 2004).
[25] M. Schuler, D. D. Bernardis, A. M. Läuchli, and P. Rabl, The vacua of dipolar cavity quantum electrodynamics, SciPost Phys. **9**, 066 (2020).
[26] M. Hertzog, M. Wang, J. Mony, and K. Börjesson, Strong light–matter interactions: a new direction within chemistry, Chem. Soc. Rev. **48**, 937 (2019).

[27] M. Ruggenthaler, D. Sidler, and A. Rubio, Understanding Polaritonic Chemistry from Ab Initio Quantum Electrodynamics, Chem. Rev. **123**, 11191 (2023).

[28] J. Flick, C. Schäfer, M. Ruggenthaler, H. Appel, and A. Rubio, Ab Initio Optimized Effective Potentials for Real Molecules in Optical Cavities: Photon Contributions to the Molecular Ground State, ACS Photonics **5**, 992 (2018).

[29] X. Gonze, D. C. Allan, and M. P. Teter, Dielectric tensor, effective charges, and phonons in α-quartz by variational density-functional perturbation theory, Phys. Rev. Lett. **68**, 3603 (1992).

[30] T. Sohier, M. Calandra, and F. Mauri, Two-dimensional Fröhlich interaction in transition-metal dichalcogenide monolayers: Theoretical modeling and first-principles calculations, Phys. Rev. B **94**, 085415 (2016).

[31] D. M. Juraschek and P. Narang, Highly Confined Phonon Polaritons in Monolayers of Perovskite Oxides, Nano Letters **21**, 5098 (2021).

[32] M. Ruggenthaler, N. Tancogne-Dejean, J. Flick, H. Appel, and A. Rubio, From a quantum-electrodynamical light–matter description to novel spectroscopies, Nat. Rev. Chem. **2**, 0118 (2018).

[33] D. M. Welakuh and P. Narang, Tunable Nonlinearity and Efficient Harmonic Generation from a Strongly Coupled Light–Matter System, ACS Photonics **10**, 383 (2023).

[34] A. Marini, Equilibrium and out-of-equilibrium realistic phonon self-energy free from overscreening, Phys. Rev. B **107**, 024305 (2023).

[35] G. Stefanucci, R. van Leeuwen, and E. Perfetto, In and Out-of-Equilibrium Ab Initio Theory of Electrons and Phonons, Phys. Rev. X **13**, 031026 (2023).

[36] J. Foley IV, J. McTague, and A. DePrince III, Ab Initio Methods for Polariton Chemistry, Chem. Phys. Rev. **4**, 041301 (2023).

[37] J. Čížek, On the Correlation Problem in Atomic and Molecular Systems. Calculation of Wavefunction Components in Ursell-Type Expansion Using Quantum-Field Theoretical Methods, J. Chem. Phys. **45**, 4256 (1966).

[38] H. Kümmel, Origins of the Coupled Cluster Method, Theoret. Chim. Acta **80**, 81 (1991).

[39] A. White, Y. Gao, A. J. Minnich, and G. Chan, A coupled cluster framework for electrons and phonons, J. Chem. Phys. **153**, 224112 (2020).

[40] U. Mordovina, C. Bungey, H. Appel, P. J. Knowles, A. Rubio, and F. R. Manby, Polaritonic coupled-cluster theory, Phys. Rev. Res. **2**, 023262 (2020).

[41] T. S. Haugland, E. Ronca, E. F. Kjønstad, A. Rubio, and H. Koch, Coupled Cluster Theory for Molecular Polaritons: Changing Ground and Excited States, Phys. Rev. X **10**, 041043 (2020).

[42] M. Liebenthal, N. Vu, and A. DePrince III, Equation-of-motion cavity quantum electrodynamics coupled-cluster theory for electron attachment, J. Chem. Phys. **156**, 054105 (2022).

[43] F. Pavošević and J. Flick, Polaritonic Unitary Coupled Cluster for Quantum Computations, J. Phys. Chem. Lett. **12**, 9100 (2021).

[44] F. Pavošević, I. Tavernelli, and A. Rubio, Spin-Flip Unitary Coupled Cluster Method: Toward Accurate Description of Strong Electron Correlation on Quantum Computers, J. Phys. Chem. Lett. **14**, 7876 (2023).

[45] M. Denner, A. Miessen, H. Yan, I. Tavernelli, T. Neupert, E. Demler, and Y. Wang, A hybrid quantum-classical method for electron-phonon systems, Commun. Phys. **6**, 233 (2023).

[46] C. L. Benavides-Riveros, L. Chen, C. Schilling, S. Mantilla, and S. Pittalis, Excitations of Quantum Many-Body Systems via Purified Ensembles: A Unitary-Coupled-Cluster-Based Approach, Phys. Rev. Lett. **129**, 066401 (2022).

[47] H. R. Grimsley, D. Claudino, S. E. Economou, E. Barnes, and N. J. Mayhall, Is the Trotterized UCCSD Ansatz Chemically Well-Defined?, J. Chem. Theory Comput. **16**, 1 (2020).

[48] D. A. Mazziotti, Contracted Schrödinger equation: Determining quantum energies and two-particle density matrices without wave functions, Phys. Rev. A **57**, 4219 (1998).

[49] F. Colmenero and C. Valdemoro, Approximating q-order reduced density matrices in terms of the lower-order ones. II. Applications, Phys. Rev. A **47**, 979 (1993).

[50] H. Nakatsuji and K. Yasuda, Direct Determination of the Quantum-Mechanical Density Matrix Using the Density Equation, Phys. Rev. Lett. **76**, 1039 (1996).

[51] D. A. Mazziotti, Comparison of contracted Schrödinger and coupled-cluster theories, Phys. Rev. A **60**, 4396 (1999).

[52] D. Mukherjee and W. Kutzelnigg, Irreducible Brillouin conditions and contracted Schrödinger equations for n-electron systems. I. The equations satisfied by the density cumulants, J. Chem. Phys. **114**, 2047 (2001).

[53] K. Yasuda, Uniqueness of the solution of the contracted Schrödinger equation, Phys. Rev. A **65**, 052121 (2002).

[54] D. A. Mazziotti, Variational method for solving the contracted Schrödinger equation through a projection of the N-particle power method onto the two-particle space, J. Chem. Phys. **116**, 1239 (2002).

[55] D. A. Mazziotti, Exact two-body expansion of the many-particle wave function, Phys. Rev. A **102**, 030802 (2020), 2010.02191.

[56] S. E. Smart and D. A. Mazziotti, Verifiably exact solution of the electronic Schrödinger equation on quantum devices, Phys. Rev. A **109**, 022802 (2024).

[57] L. Cohen and C. Frishberg, Hierarchy Equations for Reduced Density Matrices, Phys. Rev. A **13**, 927 (1976).

[58] H. Nakatsuji, Equation for the direct determination of the density matrix, Phys. Rev. A **14**, 41 (1976).

[59] C. Valdemoro, L. Tel, D. Alcoba, and E. Pérez-Romero, The contracted Schrödinger equation methodology: study of the third-order correlation effects, Theor. Chem. Account. **118**, 503 (2007).

[60] D. A. Mazziotti, Anti-Hermitian Contracted Schrödinger Equation: Direct Determination of the Two-Electron Reduced Density Matrices of Many-Electron Molecules, Phys. Rev. Lett. **97**, 143002 (2006).

[61] D. A. Mazziotti, Anti-Hermitian part of the contracted Schrödinger equation for the direct calculation of two-electron reduced density matrices, Phys. Rev. A **75**, 022505 (2007).

[62] D. A. Mazziotti, Multireference many-electron correlation energies from two-electron reduced density matrices computed by solving the anti-Hermitian contracted Schrödinger equation, Phys. Rev. A **76**, 052502 (2007).

[63] J. W. Snyder and D. A. Mazziotti, Photoexcited conversion of gauche-1,3-butadiene to bicyclobutane via a conical intersection: Energies and reduced density matrices from the anti-Hermitian contracted Schrödinger equation, J. Chem. Phys. **135**, 024107 (2011).
[64] G. Gidofalvi and D. A. Mazziotti, Direct calculation of excited-state electronic energies and two-electron reduced density matrices from the anti-Hermitian contracted Schrödinger equation, Phys. Rev. A **80**, 022507 (2009).
[65] D. R. Alcoba, C. Valdemoro, L. M. Tel, E. Peérez-Romero, and O. B. Oña, Optimized Solution Procedure of the G-Particle-Hole Hypervirial Equation for Multiplets: Application to Doublet and Triplet States, J. Phys. Chem. A **115**, 2599 (2011).
[66] J.-N. Boyn and D. A. Mazziotti, Accurate singlet–triplet gaps in biradicals via the spin averaged anti-Hermitian contracted Schrödinger equation, J. Chem. Phys. **154**, 134103 (2021).
[67] D. A. Mazziotti, Quantum Chemistry without Wave Functions: Two-Electron Reduced Density Matrices, Acc. Chem. Res. **39**, 207 (2006).
[68] D. A. Mazziotti, Contracted Schrödinger Equation, in *Reduced-Density-Matrix Mechanics: With Application to Many-Electron Atoms and Molecules* (John Wiley & Sons, Ltd, 2007) Chap. 8, pp. 165–203.
[69] D. A. Mazziotti, Two-Electron Reduced Density Matrix as the Basic Variable in Many-Electron Quantum Chemistry and Physics, Chem. Rev. **112**, 244 (2012).
[70] M. Rosina, in *Reduced Density Matrices with Applications to Physical and Chemical Systems*, edited by A. Coleman and R. Erdahl (Queen's papers in pure and applied mathematics, 1968).
[71] D. A. Mazziotti, Exactness of wave functions from two-body exponential transformations in many-body quantum theory, Phys. Rev. A **69**, 012507 (2004).
[72] S. E. Smart and D. A. Mazziotti, Quantum Solver of Contracted Eigenvalue Equations for Scalable Molecular Simulations on Quantum Computing Devices, Phys. Rev. Lett. **126**, 070504 (2021).
[73] J.-N. Boyn, A. O. Lykhin, S. E. Smart, L. Gagliardi, and D. A. Mazziotti, Quantum-classical hybrid algorithm for the simulation of all-electron correlation, J. Chem. Phys. **155**, 244106 (2021).
[74] S. E. Smart, J.-N. Boyn, and D. A. Mazziotti, Resolving correlated states of benzyne with an error-mitigated contracted quantum eigensolver, Phys. Rev. A **105**, 022405 (2022).
[75] S. E. Smart and D. A. Mazziotti, Many-fermion simulation from the contracted quantum eigensolver without fermionic encoding of the wave function, Phys. Rev. A **105**, 062424 (2022).
[76] Y. Wang and D. A. Mazziotti, Electronic excited states from a variance-based contracted quantum eigensolver, Phys. Rev. A **108**, 022814 (2023).
[77] Y. Wang, L. M. Smith, and D. A. Mazziotti, Quantum simulation of bosons with the contracted quantum eigensolver, New J. Phys. **25**, 103005 (2023).
[78] I. G. Lang and Y. A. Firsov, Kinetic Theory of Semiconductors with Low Mobility, Sov. Phys. JETP **16**, 1301 (1963).
[79] J. Schrieffer and P. Wolff, Relation between the Anderson and Kondo Hamiltonians, Phys. Rev. **149**, 491 (1966).
[80] Z. Hu, R. Xia, and S. Kais, A quantum algorithm for evolving open quantum dynamics on quantum computing devices, Sci. Rep. **10**, 3301 (2020).
[81] Y. Wang, E. Mulvihill, Z. Hu, N. Lyu, S. Shivpuje, Y. Liu, M. Soley, E. Geva, V. Batista, and S. Kais, Simulating Open Quantum System Dynamics on NISQ Computers with Generalized Quantum Master Equations, J. Chem. Theory Comput. **19**, 4851 (2023).
[82] M. Motta, C. Sun, A. Tan, M. O'Rourke, E. Ye, A. Minnich, F. Brandão, and G. Chan, Determining eigenstates and thermal states on a quantum computer using quantum imaginary time evolution, Nat. Phys. **16**, 205 (2020).
[83] S. McArdle, T. Jones, S. Endo, Y. Li, S. Benjamin, and X. Yuan, Variational ansatz-based quantum simulation of imaginary time evolution, npj Quantum Inf. **5**, 75 (2019).
[84] R. J. Bartlett, S. A. Kucharski, and J. Noga, Alternative coupled-cluster ansätze II. The unitary coupled-cluster method, Chem. Phys. Lett. **155**, 133 (1989).
[85] H. Nakatsuji, Structure of the exact wave function, J. Chem. Phys. **113**, 2949 (2000).
[86] M. Nooijen, Can the Eigenstates of a Many-Body Hamiltonian Be Represented Exactly Using a General Two-Body Cluster Expansion?, Phys. Rev. Lett. **84**, 2108 (2000).
[87] M. Motta, C. Sun, A. T. K. Tan, M. J. O'Rourke, E. Ye, A. J. Minnich, F. G. S. L. Brandão, and G. K.-L. Chan, Determining eigenstates and thermal states on a quantum computer using quantum imaginary time evolution, Nat. Phys. **16**, 205 (2020).
[88] F. A. Evangelista, G. K.-L. Chan, and G. E. Scuseria, Exact parameterization of fermionic wave functions via unitary coupled cluster theory, J. Chem. Phys. **151**, 244112 (2019).
[89] S. McArdle, T. Jones, S. Endo, Y. Li, S. C. Benjamin, and X. Yuan, Variational ansatz-based quantum simulation of imaginary time evolution, npj Quantum Inf. **5**, 75 (2019).
[90] S. E. Smart and D. A. Mazziotti, Accelerated Convergence of Contracted Quantum Eigensolvers through a Quasi-Second-Order, Locally Parameterized Optimization, J. Chem. Theory Comput. **18**, 5286 (2022).
[91] J. Nocedal and S. J. Wright, *Numerical Optimization* (Springer New York, NY, 2006).
[92] E. Jaynes and F. Cummings, Comparison of quantum and semiclassical radiation theories with application to the beam maser, Proceedings of the IEEE **51**, 89 (1963).
[93] M. Tavis and F. Cummings, Exact Solution for an N-Molecule—Radiation-Field Hamiltonian, Phys. Rev. **170**, 379 (1968).
[94] M. Tavis and F. Cummings, Approximate Solutions for an N-Molecule-Radiation-Field Hamiltonian, Phys. Rev. **188**, 692 (1969).
[95] M. Blaha, A. Johnson, A. Rauschenbeutel, and J. Volz, Beyond the Tavis-Cummings model: Revisiting cavity QED with ensembles of quantum emitters, Phys. Rev. A **105**, 013719 (2022).
[96] O. Castaños, E. Nahmad-Achar, R. López-Peña, and J. Hirsch, Analytic approximation of the Tavis-Cummings ground state via projected states, Phys. Scr. **80**, 055401 (2009).
[97] T. Gera and K. Sebastian, Effects of disorder on polaritonic and dark states in a cavity using the disordered

Tavis–Cummings model, J. Chem. Phys. **156**, 194304 (2022).

[98] D. De Bernardis, M. Jeannin, J.-M. Manceau, R. Colombelli, A. Tredicucci, and I. Carusotto, Magnetic-field-induced cavity protection for intersubband polaritons, Phys. Rev. B **106**, 224206 (2022).

[99] Y. Todorov and C. Sirtori, Intersubband polaritons in the electrical dipole gauge, Phys. Rev. B **85**, 045304 (2012).

[100] A. Köhn and A. Tajti, Can coupled-cluster theory treat conical intersections?, J. Chem. Phys. **127**, 044105 (2007).

[101] C. L. Benavides-Riveros, Y. Wang, S. Warren, and D. A. Mazziotti, Quantum simulation of excited states from parallel contracted quantum eigensolvers, New J. Phys. **26**, 033020 (2024).